JACS
JOURNAL OF THE AMERICAN CHEMICAL SOCIETY
Article
pubs.acs.org/JACS

Free-Standing, Single-Monomer-Thick Two-Dimensional Polymers through Covalent Self-Assembly in Solution

Kangkyun Baek,[†,‡] Gyeongwon Yun,[‡] Youngkook Kim,[‡] Dongwoo Kim,[‡] Raghunandan Hota,[‡] Ilha Hwang,[†,‡] Dan Xu,[‡] Young Ho Ko,[‡] Gil Ho Gu,[§] Ju Hyung Suh,[∥] Chan Gyung Park,[§,∥] Bong June Sung,[⊥] and Kimoon Kim*[,†,‡]

[†]Center for Self-assembly and Complexity, Institute for Basic Science, Pohang, 790-784, Republic of Korea

[‡]Center for Smart Supramolecules, Department of Chemistry, Division of Advanced Materials Science, [§]Department of Material Science and Engineering, and [∥]National Center for Nanomaterials Technology, Pohang University of Science and Technology, Pohang, 790-784, Republic of Korea

[⊥]Department of Chemistry, Sogang University, Seoul, 121-742, Republic of Korea

Supporting Information

ABSTRACT: The design and synthesis of two-dimensional (2D) polymers is a challenging task, hitherto achieved in solution only through the aid of a solid surface "template" or preorganization of the building blocks in a 2D confined space. We present a novel approach for synthesizing free-standing, covalently bonded, single-monomer-thick 2D polymers in solution without any preorganization of building blocks on solid surfaces or interfaces by employing shape-directed covalent self-assembly of rigid, disk-shaped building blocks having laterally predisposed reactive groups on their periphery. We demonstrate our strategy through a thiol−ene "click" reaction between $(allyloxy)_{12}$CB[6], a cucurbit[6]uril (CB[6]) derivative with 12 laterally predisposed reactive alkene groups, and 1,2-ethanedithiol to synthesize a robust and readily transferable 2D polymer. We can take advantage of the high binding affinity of fully protonated spermine (positive charges on both ends) to CB[6] to keep each individual polymer sheet separated from one another by electrostatic repulsion during synthesis, obtaining, for the first-time ever, a single-monomer-thick 2D polymer in solution. The arrangement of CB[6] repeating units in the resulting 2D polymer has been characterized using gold nanoparticle labeling and scanning transmission electron microscopy. Furthermore, we have confirmed the generality of our synthetic approach by applying it to different monomers to generate 2D polymers. Novel 2D polymers, such as our CB[6] derived polymer, may be useful in selective transport, controlled drug delivery, and chemical sensing and may even serve as well-defined 2D scaffolds for ordered functionalization and platforms for bottom-up 3D construction.

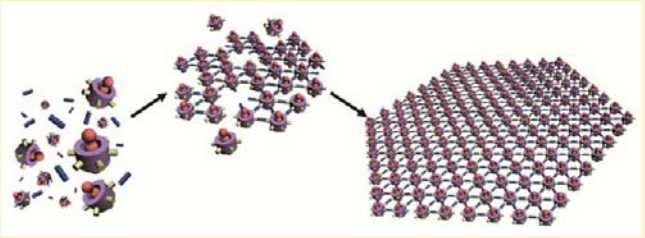

INTRODUCTION

Two-dimensional (2D) polymers can be defined as free-standing, covalently bonded, single-atom/monomer-thick films, as exemplified by graphene. Such polymers provide unique opportunities to address fundamental scientific questions and are anticipated to be useful for a wide range of technological applications, some of which would otherwise be impossible to realize.[1] Theoretical studies already anticipated unusual mechanical and folding behavior of such structures,[2] long before the exfoliation of graphite into graphene was reported.[3] Successful isolation of graphene has only intensified the bottom up synthetic efforts in recent years,[3] as these 2D polymers are further envisaged to find applications in various fields including selective transport, molecular electronics, sensors, surface catalysis, and drug delivery because of the unique spatial arrangement of functional building blocks in a single layer and their assembly.[1,4] However, the lack of a robust method to produce free-standing single-atom/monomer-thick 2D polymers as bulk material with macroscopic dimensions has, in general, hindered the investigation of their fundamental properties as well as their practical applications.[1]

Since the 1980s, there have been a number of attempts to synthesize 2D polymers through polymerization of monomers in a preorganized structure within a 2D confined space created by oil−water[5a] and air−water[5b] interfaces, a solid surface that organizes a self-ordered monolayer,[5c] or the interior of a lipid or surfactant bilayer surrounded by water.[5d,6] However, once they are isolated from the 2D confined space, the 2D structural integrity is lost due to the lack of in-plane cross-linking of monomers. Recently, surface-mediated polymerization approaches using atomically flat metal surfaces which can act as "templates",[1b] under ultrahigh vacuum (UHV) conditions or at solid−liquid interface, have been explored,[1b,7] but the resultant materials have a lateral size only in the nanometer regime and exhibit transferability issues.[1b] Ultrasonic exfoliation of 2D

Received: January 8, 2013
Published: April 10, 2013

dx.doi.org/10.1021/ja4002019 | J. Am. Chem. Soc. 2013, 135, 6523−6528

Scheme 1. Covalent Self-Assembly of 2D Polymer[a]

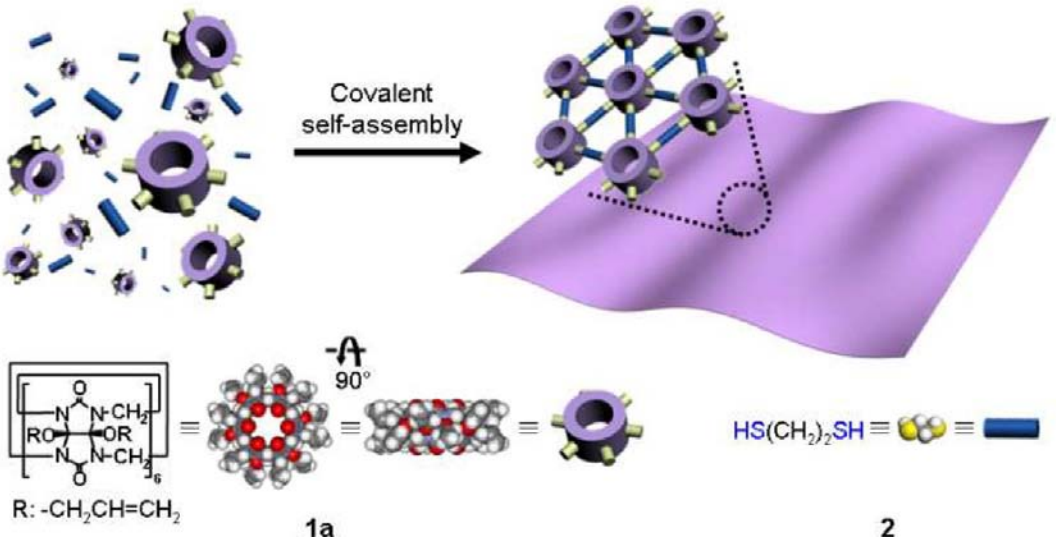

[a]Schematic representation of free-standing 2D polymer formation using $(allyloxy)_{12}$CB[6] and ethanedithiol through irreversible covalent self-assembly. Only CB[6] and thioether bridges are shown in a zoomed area of the 2D polymer.

metal–organic frameworks (MOF) into single sheets to be dispersed in solvent has also been demonstrated in recent years.[8] However, such ultrasonic exfoliation of covalent organic frameworks (COF) into individual sheets of 2D organic polymer films has not been achieved so far.[9] A successful synthesis of a 2D organic polymer was recently achieved by Sakamoto et al, which involves solid-state topochemical photocross-linking of monomers preorganized as 2D layers in a crystal and subsequent isolation of individual layers in solution from the swollen crystals.[10] However, since this monomer lacks a robust supramolecular synthon and may produce other polymorphs upon crystallization, a priori prediction of isostructure for similar molecules is not feasible. Thus, a general method based on this approach is far from ideal. Overall, despite the recent progress, the synthesis of 2D structures still requires preorganization of monomers into 2D geometries prior to cross-linking with the assistance of secondary substrates or interfaces, and the preparation of 2D polymers in solution without the aid of any solid surfaces, interfaces, or preorganization of monomers has not yet been achieved.

Herein, we report a facile solution-phase synthesis of readily transferable 2D organic polymers in the micrometer lateral size regime only through shape-directed covalent self-assembly and without any preorganization of building blocks by means of solid surfaces or interfaces. We have found that lateral cross-linking of various rigid and disk-shaped monomers having multiple in-plane reactive groups at the periphery results in the predominant lateral growth of polymers. Furthermore, for a specific monomer, we have also achieved the synthesis of a free-standing single-layer 2D polymer by exploiting the monomer's ability to tightly bind a thread-like guest molecule having positive charges on both ends, which keeps each individual polymer sheet separated from another by electrostatic repulsion during the synthesis. Overall, this new solution-phase approach may enable a convenient, mass production of readily transferable 2D polymers.

RESULTS AND DISCUSSION

Rationale behind Our Approach to the Synthesis of 2D Polymers in Solution. Recently, we discovered the spontaneous formation of polymer nanocapsules[11] in solution by thiol–ene "click" reaction[12] between $(allyloxy)_{12}$cucurbit[6]uril[13] **1a** (Scheme 1), a disk-shaped macrocycle with 12 alkene groups laterally predisposed around a rigid cucurbit[6]uril (CB[6]) core capable of binding alkyl ammonium ions tightly,[14] and various dithiol linkers without the help of any physical surface or interface acting as a "template" or preorganization of the monomers. We further confirmed the generality of the nanocapsule formation for various disk-shaped monomers having multiple polymerizable groups in their periphery.[15] It should be noted that this is a rare example of covalent self-assembly through irreversible covalent bond formation.[11] During a mechanistic study of the nanocapsule formation, we observed small 2D oligomeric patches as intermediates, which then turned into larger curved objects, followed by further reaction to form hollow polymer nanocapsules.[11b] Theoretical studies suggested that low bending rigidity of building blocks and a poor solvent would encourage the generation of curvature in the intermediates, whereas high bending rigidity and a good solvent would allow the lateral growth of the intermediates without bending.[11b] Indeed, when using *N*,*N*-dimethyformamide (DMF) as solvent, we noticed the formation of certain rolled or folded objects instead of nanocapsules and later confirmed as multilayered polymer films after treatment of methanol (Figure 1a).

Encouraged by this result, we decided to develop a facile and general method to synthesize free-standing, covalently bonded, 2D organic polymers in solution without the aid of any solid surfaces or interfaces by using (1) rigid and disk-shaped building blocks having laterally predisposed reactive groups at the periphery; (2) short linkers for high-bending rigidity, if necessary; and (3) careful choice of appropriate solvents which would lead to rigid and better soluble intermediates and allow them to remain flat as they grow into 2D polymers with macroscopic lateral dimensions and molecular-scale thickness.

Synthesis and Characterization of 2D Polymers. The synthesis of free-standing 2D polymer **3a** was achieved in solution via the thiol–ene photopolymerization of $(allyloxy)_{12}$CB[6] **1a** and 1,2-ethandithiol **2** without any

dx.doi.org/10.1021/ja4002019 | J. Am. Chem. Soc. 2013, 135, 6523–6528

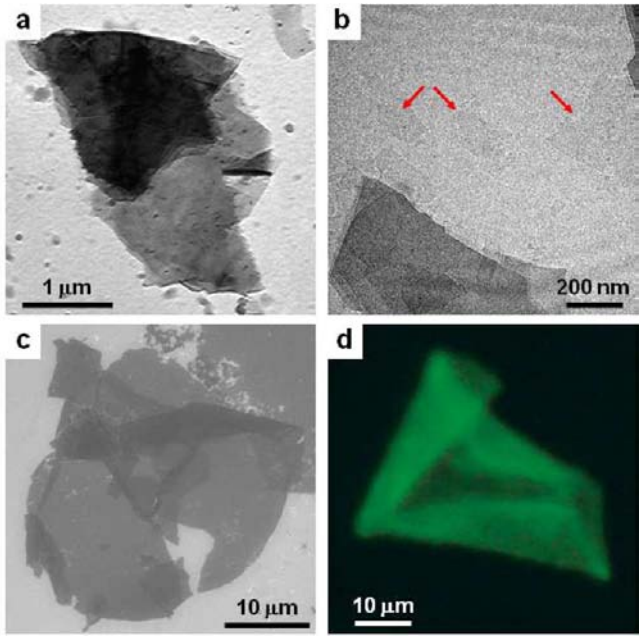

Figure 1. Various microscopic images of thin polymer films. (a) TEM image of unrolled and stacked polymer films synthesized in DMF. (b) TEM image of **3a** synthesized in DMA and the red arrows indicate the presence of individual thin films. (c) SEM image of **3a** synthesized in DMA. (d) FM image of **3a** decorated with FITC spermidine by taking advantage of strong host–guest interaction between CB[6] and protonated spermidine (Figure S11).

assistance of solid surfaces or interfaces (Scheme 1). In a typical experiment, a mixture solution of **1a** and **2** in a 1:48 ratio (alkene: thiol = 1: 8) in *N*,*N*-dimethylacetamide (DMA), a more solubilizing solvent than the previously used DMF, was irradiated with UV for 6 h. Subsequently, ethyl vinyl ether was added to terminate the thiol–ene reaction by removal of remaining free thiol groups and disulfide loops made of dithiol linkers[16] followed by dialysis. The reaction produced 2D polymer **3a** in 78% yield based on **1a** (See Supporting Information). The FT-IR spectrum of **3a** showed two characteristic peaks (blue dotted line in Figure S2) of the CB[6] unit of **1a** at 1765 and 1457 cm^{-1} corresponding to the C═O and C–N stretching vibrations and decreased in intensity of the alkene peaks (red dotted line in Figure S2) of **1a**. The solid-state ^{13}C NMR spectrum of **3a** also revealed almost complete disappearance of the alkene peaks of **1a** at 120 and 136 ppm as well as appearance of a thioether peak at 30 ppm, which confirms the formation of new thioether bridges and disappearance of the allyl groups (Figure S3).

Since **1a** composed of C, H, O, N atoms and **2** composed of C, H, S atoms are the only sources for nitrogen and sulfur atoms, respectively, we reasoned that the N/S ratio of **3a** may provide a clue to the composition and structure of the polymer network constituting the 2D polymer. Elemental analysis showed that the ratio of **1a** and **2** incorporated in **3a** is 1:9.2. This suggested that upon reacting with **2**, approximately 6 of the 12 alkene groups of **1a** form thioether bridges with a composition of $-O(CH_2)_3-S(CH_2)_2S-(CH_2)_3O-$, which link neighboring CB[6] units to yield a 2D polymer network (green line in Figure S1).[17] It also suggested that the remaining six alkene groups of **1a** formed dangling arms with a composition of $-O(CH_2)_3-S(CH_2)_2S-(CH_2)_2OCH_2CH_3$ after the reaction with **2** followed by the ethyl vinyl ether treatment (See Supporting Information). These arms presumably fill the interstitial space between neighboring CB[6] units of the 2D polymer (red line in Figure S1).

The ready transferability of **3a** in solution enabled us to characterize it by various microscopic techniques. Transmission electron microscopy (TEM) analysis of **3a** revealed the presence of thin 2D polymer films (Figure 1b), several of them stacked

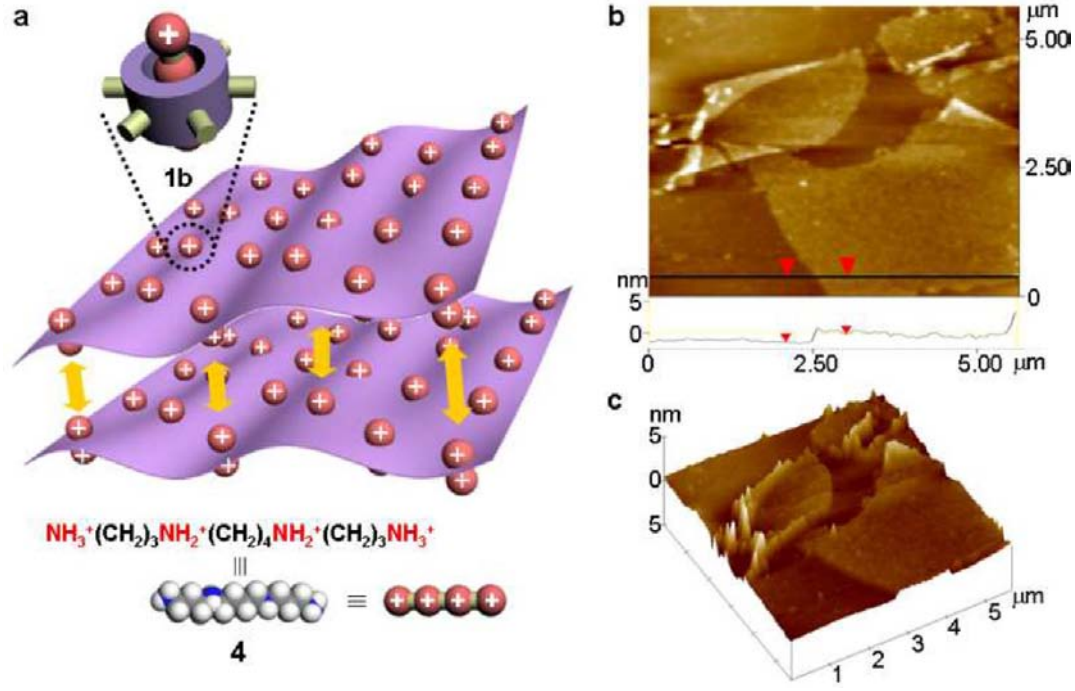

Figure 2. Single-monomer-thick 2D polymers. (a) Layer-to-layer separation through the Coulomb repulsion of 2D polymers in which each CB[6] repeating unit is threaded with protonated spermine carrying positive charges on both ends. (b) Top- and (c) perspective-view AFM images of single-monomer-thick 2D polymer **3b**.

dx.doi.org/10.1021/ja4002019 | *J. Am. Chem. Soc.* 2013, 135, 6523–6528

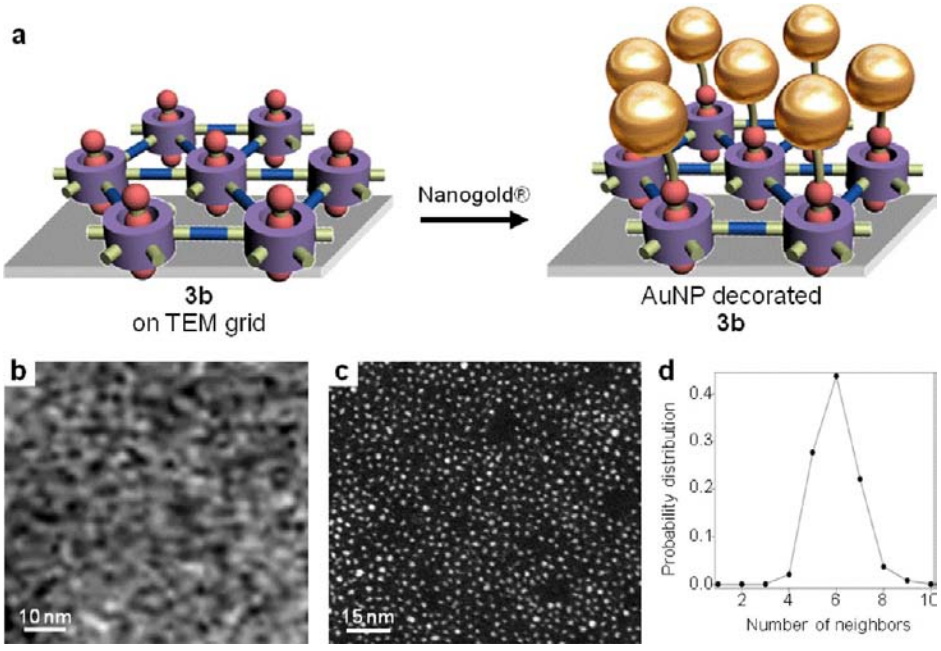

Figure 3. Network structure of 2D polymers. (a) Decoration of 2D polymers with mono-sulfo-NHS-nanogold, 1.4 nm AuNP with a single reactive sulfo-*N*-hydroxysuccinimide ester. HAADF STEM images of (b) pristine **3b** at a cryogenic temperature and (c) AuNP-labeled 2D polymers. Each white spot indicates AuNPs. (d) Probability distribution of the number of neighboring AuNPs on 2D polymers.

over each other, in lateral dimensions ranging from submicro- to several micrometers, along with a few individual thin films. Scanning electron microscopy (SEM) and fluorescence microscopy (FM) images also confirmed sheet-like polymer films with partially folded and stacked regions (Figure 1c,d). Optical microscopy images demonstrated that the films are mechanically stable enough to span over 47×47 μm^2-sized holes (Figure S5), presumably as the result of a highly cross-linked polymer network. A dynamic light scattering measurement confirmed that the observed 2D structures exist also in solution and are not simple aggregate or self-assembled species formed on the solid supports during sample preparations (Figure S6).

Formation of Single-Monomer-Thick 2D Polymer Films. We analyzed the 2D polymers with atomic force microscopy (AFM). The section analysis of AFM image of **3a** revealed that its thickness is around 2.8 nm (Figure S12), which is almost 3 times thicker than that of a single-layered 2D polymer anticipated based on modeling (Figure S14). Although resulting 2D polymer **3a** is not single-monomer thick, the high aspect ratio (>1:1000) suggested that the multiple in-plane reactive groups of the disk-shaped monomer (**1a**) likely directed the lateral growth of the polymer as single-layered films, which then turned into multilayered films due to their high propensity to stack. Unfortunately, attempts to exfoliate the films to produce single-layered 2D polymer were not successful.

Instead, to achieve single-monomer-thick polymer films, we decided to use a strong host−guest complex (**1b**) of $(allyloxy)_{12}$CB[6] and protonated spermine (**4**), a thread-like molecule having four positive ammonium groups,[14] which may allow the layer-to-layer separation of polymer films through the Coulomb repulsion during polymerization with **2** (Figures 2a and S14). Indeed, under the same conditions, the polymerization of **1b** with **2** produced single-monomer-thick 2D polymers **3b** in 70% yield.[18] The AFM image of **3b** showed the average thickness to be 2.0 ± 0.1 nm (Figure 2b,c), which is comparable to the height of **1b** (~1.5 nm) accounting for counterions (Cl^-) and possibly a water layer.[14] For the same reason, the heights of double- and triple-layer regions (5.5 and 9.5 nm, respectively) of folded films are slightly higher than the calculated values (Figure S16).

Network Structure of 2D Polymers. Having successfully synthesized the single-monomer-thick polymer films, we turned our attention to the network structure of the 2D polymer. High-resolution imaging of the network structure of pristine **3b** was hampered by the extremely electron-beam sensitive nature of the single-layered polymer films. Despite our significant efforts with high angle annular dark field (HAADF) scanning transmission electron microscopy (STEM) at a cryogenic temperature, the micrographs revealed only with limited resolution the spatial arrangement of individual CB[6] (Figure 3b). We thus decided to tackle this problem in an indirect way. We first tagged 1.4 nm gold nanoparticles (AuNP) on the 2D polymer by treating **3b** on TEM sample grid with mono-sulfo-NHS-nanogold (Nanoprobes, Inc.) to anchor one AuNP on the terminal of each protonated spermine threaded in CB[6] and visualized AuNPs by STEM (Figures 3a and S17).[19] Although some "defect" sites are evident, the HAADF-STEM image revealed that the AuNPs are more or less uniformly distributed on the 2D polymers (Figure 3c), whereas there is no significant adsorption of AuNPs bearing no sulfo-NHS functionality on 2D polymer films **3b** (Figure S18). The "defects" may be due to the irreversible nature of the thiol−ene click reaction used in polymerization step or incomplete anchoring of AuNPs on the terminal of protonated spermine threaded CB[6] units. A distribution analysis indicated that each AuNP is surrounded by ~6 AuNPs on average (Figure 3d), and the average distance between neighboring AuNPs is around 3 nm (Figure S19), which matches reasonably well with the calculated distance between neighboring CB[6] units (~2.9 nm) based on an ideal hexagonal arrangement of the monomer units in the 2D polymer. In addition, elemental analysis suggested that each CB[6] unit in **3a** makes six thioether bridges to neighboring CB[6] units to yield a 2D polymer network (See

dx.doi.org/10.1021/ja4002019 | *J. Am. Chem. Soc.* 2013, 135, 6523−6528

Supporting Information). Taken together, these results suggest that the 2D polymer **3b** has a quasihexagonal network structure with some defects due, at least in part, to the irreversible nature of the thiol−ene click reaction used in the polymerization step.

Monte Carlo Simulations of Covalent Network Growth. To elucidate the effect of the number and position of reactive groups on the building block on the formation of 2D polymers, we performed Monte Carlo simulations.[20] To simplify the problem, we used a hard sphere as a building block, attached a varying number of reactive groups in different positions, and examined how the spheres assemble into a polymer. The simulation showed that the dimensionality of the resulting polymer network is predominantly determined not only by the number of reactive groups in the building block but also by their spatial disposition (Figure S20). For instance, spheres with six reactive groups evenly attached on the equator produce a 2D hexagonal network, whereas their arrangement in octahedral symmetry produces a polymer with a 3D network. This result suggests that the geometric aspects of building block, i.e., multiple sticky groups in the same plane of a rigid core, may be one of the most important factors governing the formation of 2D structures.

2D Polymers from Other Rigid Building Blocks. To test the simulation results and the generality of our solution phase approach without any aid of solid surfaces or interfaces, we carried out a preliminary study for the formation of 2D polymers using other monomers having a flat rigid core with multiple in-plane reactive groups at the periphery. The thiol−ene photopolymerization of a triphenylene derivative (**5**), having six allyloxy groups, with **2** in DMA (Figure S1b) successfully produced micrometer-sized thin polymer film **6** (Figure S21).[21] In addition, olefin cross-metathesis reaction of a zinc-phthalocyanine derivative (**7**), having eight terminal olefin groups, with Grubbs' catalyst (Figure S1c) also produced micrometer-sized thin polymer film **8** (Figure S22). The polymer films **6** and **8** were much thicker (∼4.5 and ∼4.8 nm, respectively) than the expected single-layer 2D polymers of **5** and **7** (Figure S21f and S22f), once again presumably as a result of multiple stacking of 2D polymers due to the strong $\pi-\pi$ interactions (Figure S24) between the layers.[22] However, the aspect ratio of the resulting films is about 1:1000, which strongly supports the predominant lateral growth of polymer films. Despite considerable efforts, attempts to exfoliate the films to produce single-layer 2D polymer have been unsuccessful so far. Nevertheless, these simulation and experimental results suggest that our approach to 2D polymers may be applicable to other building blocks with a flat core and multiple in-plane reactive groups at the periphery, apart from $(allyloxy)_{12}CB[6]$. Further studies along this line are in progress.

Polymerization with Out-of-Plane Reactive Groups. To test how out-of-plane reactive groups in monomers affect polymerization, we introduced an allyl group at each end of the protonated spermine and let it form a tight 1:1 host−guest complex (**1c**) with **1a**. Indeed, under the same conditions, the polymerization of **1c** with **2** produced a 3D random polymer rather than a 2D polymer (Figure S26), which is consistent with the simulation results. Both simulation and experimental results suggested that the number as well as the location of reactive groups is a key factor for the formation of a 2D network structure.

CONCLUSIONS

We have demonstrated a novel approach to synthesize free-standing, readily transferable, single-monomer-thick 2D organic polymers via shape-directed covalent self-assembly in solution without using any template or preorganized structure. The multiple reactive alkene groups in $(allyloxy)_{12}CB[6]$ resulted in a robust 2D polymer upon clicking with a dithiol linker in an appropriate solvent. Furthermore, by exploiting the exceptionally high binding affinity of CB[6] with protonated spermine, a molecular thread with positive charges on both ends, we successfully obtained single-monomer-thick layers of the resulting 2D polymer with individual CB[6] cores in the 2D polymer arranged in a quasihexagonal structures. Remarkably, as suggested by our preliminary results, our synthetic approach appears to be applicable to other monomers and thus may represent a general strategy for synthesizing 2D polymers in the absence of an external physical templating surface/interface. Furthermore, 2D polymers such as that formed from CB[6] can readily be functionalized due to its accessible pores; such structures may find useful applications in many diverse areas including selective transport, controlled drug delivery, and chemical sensing and can also potentially act as well-defined 2D scaffolds for ordered functionalization or platforms for bottom-up 3D construction.

ASSOCIATED CONTENT

Supporting Information

General procedure and materials; synthesis of free-standing 2D polymer **3a** and **3b**; possible arrangement of CB[6] units in **3a** and **3b**; monitoring of formation of **3a** at various reaction time points; surface modification of **3a** with nanogold; synthesis of **1b**, **1c**, **6**, **8**, diallyl-spermine **9**, and **3c**; surface decoration of **3b** with nanogold; Monte Carlo simulation; schematic representation of the formation of 2D polymer **3a**, **6**, and **8**; FT-IR spectra of **1a** and **3a**; solid state ^{13}C NMR spectra of **1a** and **3a**; TEM images of **3a** and **3b**; OM image of **3a**; size distribution and TEM images of **3b** in DMA before and after treatment of TCEP; TEM and AFM images of **3b** without termination reaction; FT-IR spectra and TEM images of **3a** at various reaction time points; FM images of FITC-modified **3a**; AFM images of **3a**; schematic representation of interlayer cross-linking; pictorial representation of **3a**, **1b**, and **3b**; ^{1}H NMR and DOSY NMR spectra of **1b**; AFM images and height profiles of **3b**; schematic representation of AuNP labeling; TEM images after treating **3b** with AuNPs bearing no sulfo-NHS functionality; histogram of observed spacings; representative snapshots of Monte Carlo simulation; TEM and AFM images of 2D polymer **6** and **8**; SEM and TEM images of polymerization of **5** using different dithiols; UV−vis absorption spectra of **6** and **8**; photograph of dialyzed solution of **3b**, **6**, and **8**; SEM and TEM images of **3c**. This material is available free of charge via the Internet at http://pubs.acs.org.

AUTHOR INFORMATION

Corresponding Author

kkim@postech.ac.kr

Notes

The authors declare no competing financial interest.

ACKNOWLEDGMENTS

This work was supported by Research Center Program (project no. CA1203) of Institute for Basic Science (IBS), Acceleration Research, Brain Korea 21, and World Class University (project no. R31-2008-000-10059-0) in Korea. We thank Dr. Ramalingam Natarajan and Mr. J. Mark Kim for helpful discussions,

Dr. Nam-Suk Lee for TEM experiments, and the support of FEI Company (NanoPort, Eindhoven).

REFERENCES

(1) (a) Geim, A. K.; Novoselov, K. S. *Nat. Mater.* **2007**, *6*, 183−191. (b) Perepichka, D. F.; Rosei, F. *Science* **2009**, *323*, 216−217. (c) Sakamoto, J.; van Heijst, J.; Lukin, O.; Schlüter, A. D. *Angew. Chem., Int. Ed.* **2009**, *48*, 1030−1069. (d) Mas-Ballesté, R.; Gómez-Navarro, C.; Gómez-Herrero, J.; Zamora, F. *Nanoscale* **2011**, *3*, 20−30. (e) Wang, Y.; Wang, X.; Antonietti, M. *Angew. Chem., Int. Ed.* **2012**, *51*, 68−89. (f) Chen, L.; Hernandez, Y.; Feng, X.; Müllen, K. *Angew. Chem., Int. Ed.* **2012**, *51*, 7640−7654.

(2) (a) Kantor, Y.; Kardar, M.; Nelson, D. R. *Phys. Rev. Lett.* **1986**, *57*, 791−794. (b) Kantor, Y.; Kardar, M.; Nelson, D. R. *Phys. Rev. A* **1987**, *35*, 3056−3071. (c) Abraham, F. F.; Nelson, D. R. *J. Phys. (Paris)* **1990**, *51*, 2653−2672. (d) Abraham, F. F.; Nelson, D. R. *Science* **1990**, *249*, 393−397. (e) Abraham, F. F.; Kardar, M. *Science* **1991**, *252*, 419−422. (f) Spector, M. S.; Naranjo, E.; Chiruvolu, S.; Zasadzinski, J. A. *Phys. Rev. Lett.* **1994**, *73*, 2867−2870.

(3) (a) Novoselov, K. S.; Geim, A. K.; Morozov, S. V.; Jiang, D.; Zhang, Y.; Dubonos, S. V.; Grigorieva, I. V.; Firsov, A. A. *Science* **2004**, *306*, 666−669. (b) Novoselov, K. S.; Jiang, D.; Schedin, F.; Booth, T. J.; Khotkevich, V. V.; Morozov, S. V.; Geim, A. K. *Proc. Natl. Acad. Sci. U.S.A.* **2005**, *102*, 10451−10453. (c) Zhang, Y.; Tan, T.-W.; Stormer, H. L.; Kim, P. *Nature* **2005**, *438*, 201−204.

(4) (a) Howorka, S.; Siwy, Z. *Chem. Soc. Rev.* **2009**, *38*, 2360−2384. (b) Jiang, D.; Cooper, V. R.; Dai, S. *Nano Lett.* **2009**, *9*, 4019−4024. (c) Makiura, R.; Motoyama, S.; Umemura, Y.; Yamanaka, H.; Sakata, O.; Kitagawa, H. *Nat. Mater.* **2010**, *9*, 565−571.

(5) (a) Rehage, H.; Schnabel, E.; Veyssie, M. *Macromol. Chem. Phys.* **1988**, *189*, 2395−2408. (b) Day, D.; Hub, H.-H.; Ringsdorf, H. *Isr. J. Chem.* **1979**, *18*, 325−329. (c) Wu, J.; Harwell, J. H.; O'Rear, E. A. *Langmuir* **1987**, *3*, 531−537. (d) Regen, S. L.; Shin, J.-S.; Yamaguchi, K. *J. Am. Chem. Soc.* **1984**, *106*, 2446−2447.

(6) (a) Stupp, S. I.; Son, S.; Lin, H. C.; Li, L. S. *Science* **1993**, *259*, 59−63. (b) Stupp, S. I.; Son, S.; Li, L. S.; Lin, H. C.; Keser, M. *J. Am. Chem. Soc.* **1995**, *117*, 5212−5227.

(7) (a) Grill, L.; Dyer, M.; Lafferentz, L.; Persson, M.; Peters, M. V.; Hecht, S. *Nat. Nanotechnol.* **2007**, *2*, 687−691. (b) Bieri, M.; Treier, M.; Cai, J.; Aït-Mansour, K.; Ruffieux, P.; Gröning, O.; Gröning, P.; Kastler, M.; Rieger, R.; Feng, X.; Müllen, K.; Fasel, R. *Chem. Commun.* **2009**, *45*, 6919−6921. (c) Cai, J.; Ruffieux, P.; Jaafar, R.; Bieri, M.; Braun, T.; Blankenburg, S.; Muoth, M.; Seitsonen, A. P.; Saleh, M.; Feng, X.; Müllen, K.; Fasel, R. *Nature* **2010**, *466*, 470−473. (d) Bieri, M.; Nguyen, M.-T.; Gröning, O.; Cai, J.; Treier, M.; Aït-Mansour, K.; Ruffieux, P.; Pignedoli, C. A.; Passerone, D.; Kastler, M.; Müllen, K.; Fasel, R. *J. Am. Chem. Soc.* **2010**, *132*, 16669−16676. (e) Treier, M.; Pignedoli, C. A.; Laino, T.; Rieger, R.; Müllen, K. *Nat. Chem.* **2011**, *3*, 61−67. (f) Bieri, M.; Blankenburg, S.; Kivala, M.; Pignedoli, C. A.; Ruffieux, P.; Müllen, K.; Fasel, R. *Chem. Commun.* **2011**, *47*, 10239−10241. (g) Abel, M.; Clair, S.; Ourdjini, O.; Mossoyan, M.; Porte, L. *J. Am. Chem. Soc.* **2011**, *133*, 1203−1205. (h) Tanoue, R.; Higuchi, R.; Enoki, N.; Miyasato, Y.; Uemura, S.; Kimizuka, N.; Stieg, A. Z.; Gimzewski, J. L.; Kunitake, M. *ACS Nano* **2011**, *5*, 3923−3929.

(8) (a) Li, P.-Z.; Maeda, Y.; Xu, Q. *Chem. Commun.* **2011**, *47*, 8436−8438. (b) Tan, J.-C.; Saines, P. J.; Bithell, E. G.; Cheetham, A. K. *ACS Nano* **2012**, *6*, 615−621. (c) Marti-Gastlaldo, C.; Warren, J. E.; Stylianou, K. C.; Flack, N. L. O.; Rosseinsky, M. J. *Angew. Chem., Int. Ed.* **2012**, *51*, 11044−11048.

(9) (a) Berlanga, I.; Ruiz-González, M. L.; González-Calbet, J. M.; Fierro, J. L. G.; Mas-Ballesté, R.; Zamora, F. *Small* **2011**, *7*, 1207−1211. (b) Colson, J. W.; Woll, A. R.; Mukherjee, A.; Levendorf, M. P.; Spitler, E. L.; Shields, V. B.; Spencer, M. G.; Park, J.; Dichtel, W. R. *Science* **2011**, *332*, 228−231. (c) Feng, X.; Ding, X.; Jiang, D. *Chem. Soc. Rev.* **2012**, *41*, 6010−6022.

(10) Kissel, P.; Erni, R.; Schweizer, W. B.; Rossell, M. D.; King, B. T.; Bauer, T.; Götzinger, S.; Schlüter, A. D.; Sakamoto, J. *Nat. Chem.* **2012**, *4*, 287−291.

(11) (a) Kim, D.; Kim, E.; Kim, J.; Park, K. M.; Baek, K.; Jung, M.; Ko, Y. H.; Sung, W.; Kim, H. S.; Suh, J. H.; Park, C. G.; Na, O. S.; Lee, D.-k.; Lee, K. E.; Han, S. S.; Kim, K. *Angew. Chem., Int. Ed.* **2007**, *46*, 3471−3474. (b) Kim, D.; Kim, E.; Lee, J.; Hong, S.; Sung, W.; Lim, N.; Park, C. G.; Kim, K. *J. Am. Chem. Soc.* **2010**, *132*, 9908−9919.

(12) (a) Dondoni, A. *Angew. Chem., Int. Ed.* **2008**, *47*, 8995−8997. (b) Hoyle, C. E.; Bowman, C. N. *Angew. Chem., Int. Ed.* **2010**, *49*, 1540−1573. (c) Cramer, N. B.; Reddy, S. K.; Cole, M.; Hoyle, C.; Bowman, C. N. *J. Polym. Sci. Part A* **2004**, *42*, 5817−5826. (d) Killops, K. L.; Campos, L. M.; Hawker, C. J. *J. Am. Chem. Soc.* **2008**, *130*, 5062−5064.

(13) Jon, S. Y.; Selvapalam, N.; Oh, D. H.; Kang, J.-K.; Kim, S.-Y.; Jeon, Y. J.; Lee, J. W.; Kim, K. *J. Am. Chem. Soc.* **2003**, *125*, 10186−10187.

(14) Kim, Y.; Kim, H.; Ko, Y. H.; Selvapalam, N.; Rekharsky, M. V.; Inoue, Y.; Kim, K. *Chem.—Eur. J.* **2009**, *15*, 6143−6151.

(15) (a) Kim, E.; Kim, D.; Jung, H.; Lee, J.; Paul, S.; Selvapalam, N.; Yang, Y.; Lim, N.; Park, C. G.; Kim, K. *Angew. Chem., Int. Ed.* **2010**, *49*, 4405−4408. (b) Hota, R.; Baek, K.; Yun, G.; Kim, Y.; Jung, H.; Park, K. M.; Yoon, E.; Joo, T.; Kang, J.; Park, C. G.; Bae, S. M.; Ahn, W. S.; Kim, K. *Chem. Sci.* **2013**, *4*, 339−344.

(16) The addition of ethyl vinyl ether is not directly related to the formation of 2D structures similar to the formation of hollow nanocapsules.[9] However, it helps to prevent the formation of intra- or interlayer disulfide bonds after completion of the reaction and during the characterization (Figure S8).

(17) After treating a dispersion solution of 2D polymer with an excess amount of tris-(2-carboxyethyl) phosphine hydrochloride as a reducing agent, we have confirmed that large polymer species still exist in solution by DLS and TEM studies, which supports that most of the 2D polymer network was cross-linked through thioether bridges, not disulfide bonds (Figures S6 and S7).

(18) The host−guest complex of **1a** and spermine is stable enough to maintain its identity in DMA, as confirmed by ^{1}H NMR and DOSY NMR spectra of **1b** (Figure S15).

(19) Wang, Q.; Lin, T.; Tang, L.; Johnson, J. E.; Finn, M. G. *Angew. Chem., Int. Ed.* **2002**, *41*, 459−462.

(20) (a) Whitelam, S.; Geissler, P. L. *J. Chem. Phys.* **2007**, *127*, 154101. (b) Mondal, J.; Sung, B. J.; Yethiraj, A. *J. Chem. Phys.* **2010**, *132*, 065103.

(21) As a part of the preliminary study, we have tested the effect of the chain length of linkers on the formation of 2D polymers. Interestingly, the polymerization of **5** using longer dithiol linkers compared to 1,2-ethanedithiol produced random-shaped polymers rather than 2D sheets (Figure S23).

(22) We think that after the lateral growth of monomers **5** and **7** in two dimensions in the early stages, the resulting 2D polymers might stack over each other presumably due to the strong $\pi-\pi$ interactions between the layers and to the reduced solubility of polymeric patches as a result of polymer growth. Once the layers are stacked, some interlayer cross-linking between the stacked 2D polymers might occur on account of the proximity of the remaining reactive groups. Despite considerable efforts, all attempts to exfoliate the multilayered thin films of **6** and **8** have been unsuccessful, which may be due to the interlayer cross-linking as well as strong $\pi-\pi$ interactions. The formation of thicker films (~4−5 nm) for **6** and **8** compared to **3a** (~2.8 nm) may be explained by their much higher propensity of stacking due to strong $\pi-\pi$ interactions.